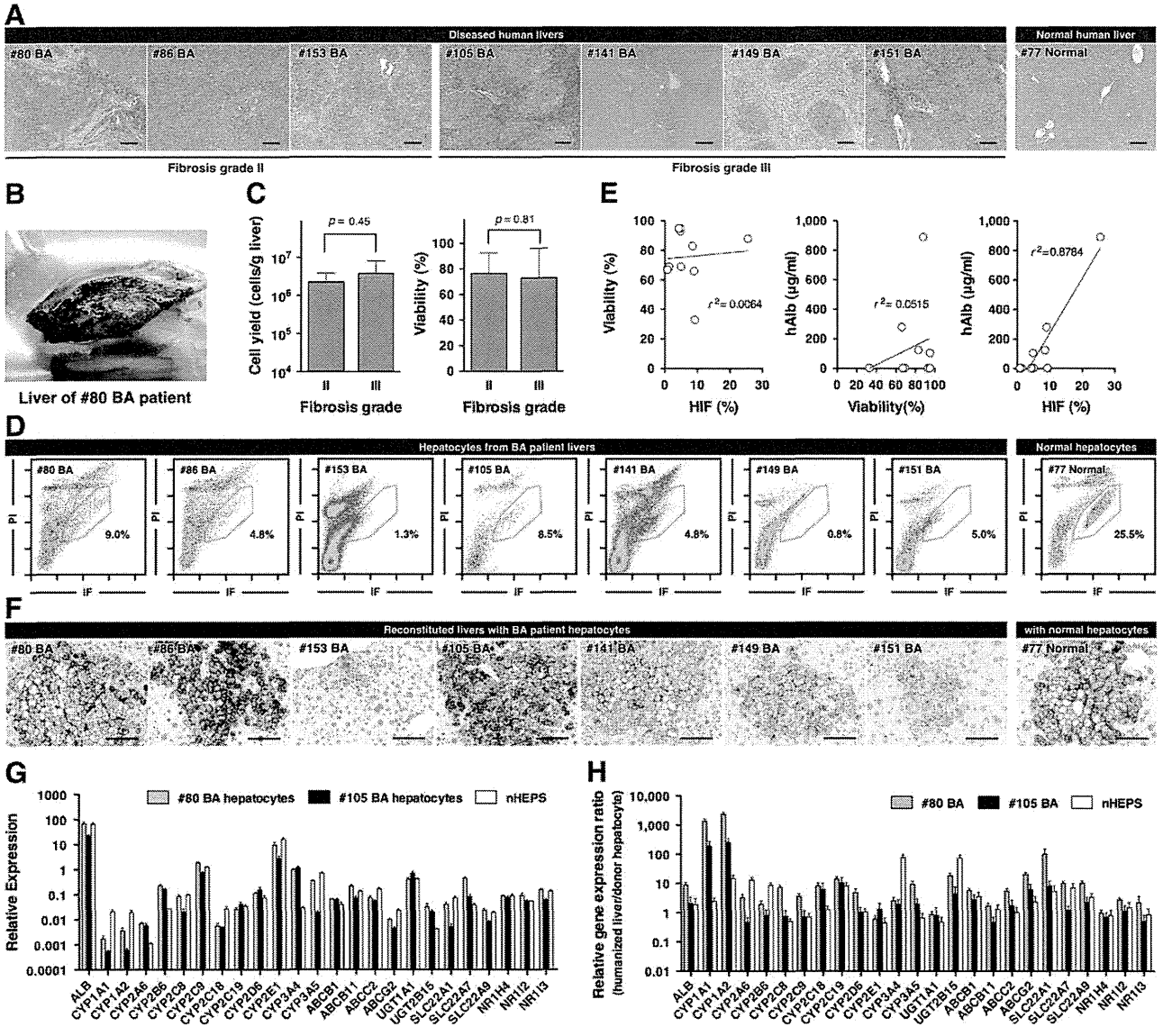

Figure 1. Engraftment of hepatocytes from BA patients in uPA-NOG mouse livers. (A) Azan-Mallory staining of 7 individual liver biopsy samples from BA patients and a healthy donor (normal). The scale bars represent 200 μm. (B) Gross morphology of the liver from BA patient 80. (C) Comparison of the cell yields and viability with grade II hepatic fibrosis and grade III hepatic fibrosis. (D) Isolated hepatocytes were analyzed with flow cytometry. Each HIF fraction is surrounded by a magenta border. (E) Correlation analyses of the cell viability, the HIF fraction percentage, and the hALB plasma concentration. (F) The engraftment of hepatocytes isolated from the BA patients and the healthy donors was confirmed with anti-human HLA staining. The scale bars represent 50 μm. (G) The relative expression levels of 24 human drug metabolism–related messenger RNAs in hepatocytes from BA patients and NHEPS hepatocytes were corrected with GAPDH. (H) The relative ratio of the gene expression for each reconstituted liver was referenced to the RNA extracted from the donor hepatocytes.

(Fig. 3A,B,). The cholestasis, visualized with Hall's bilirubin staining, was observed in many BCs in the livers of patients with BA (Fig. 3A, right). In contrast, the colonies repopulated with hepatocytes from patients with BA within the host mouse livers did not accumulate bile within their BCs (Fig. 3B). Azan-Mallory staining and VIM and αSMA antibody staining revealed fibrosis in the livers of patients with BA (Fig. 3C), but no fibrosis was observed within the colony repopulated with hepatocytes from patients with BA (Fig. 3D). We wondered whether these hepatocytes could reconstitute the functionally integrated BC network within the host mouse liver; therefore, we assessed the transporter function within the colonies of hepatocytes from patients with BA with 5-CFDA, a fluorescent marker used to visualize biliary excretion into BCs. After it is administered, 5-CFDA enters hepatocytes and is metabolized into 5-CF. This compound is excreted into BCs through the organic anion transporter MRP2.[27] Within the first 15 minutes after the administration of 5-CFDA, the hepatocytes from patients with BA in the uPA-NOG mice excreted 5-CF into the BCs, and it formed honeycomb networks surrounding individual hepatocytes (Fig. 4, top). This

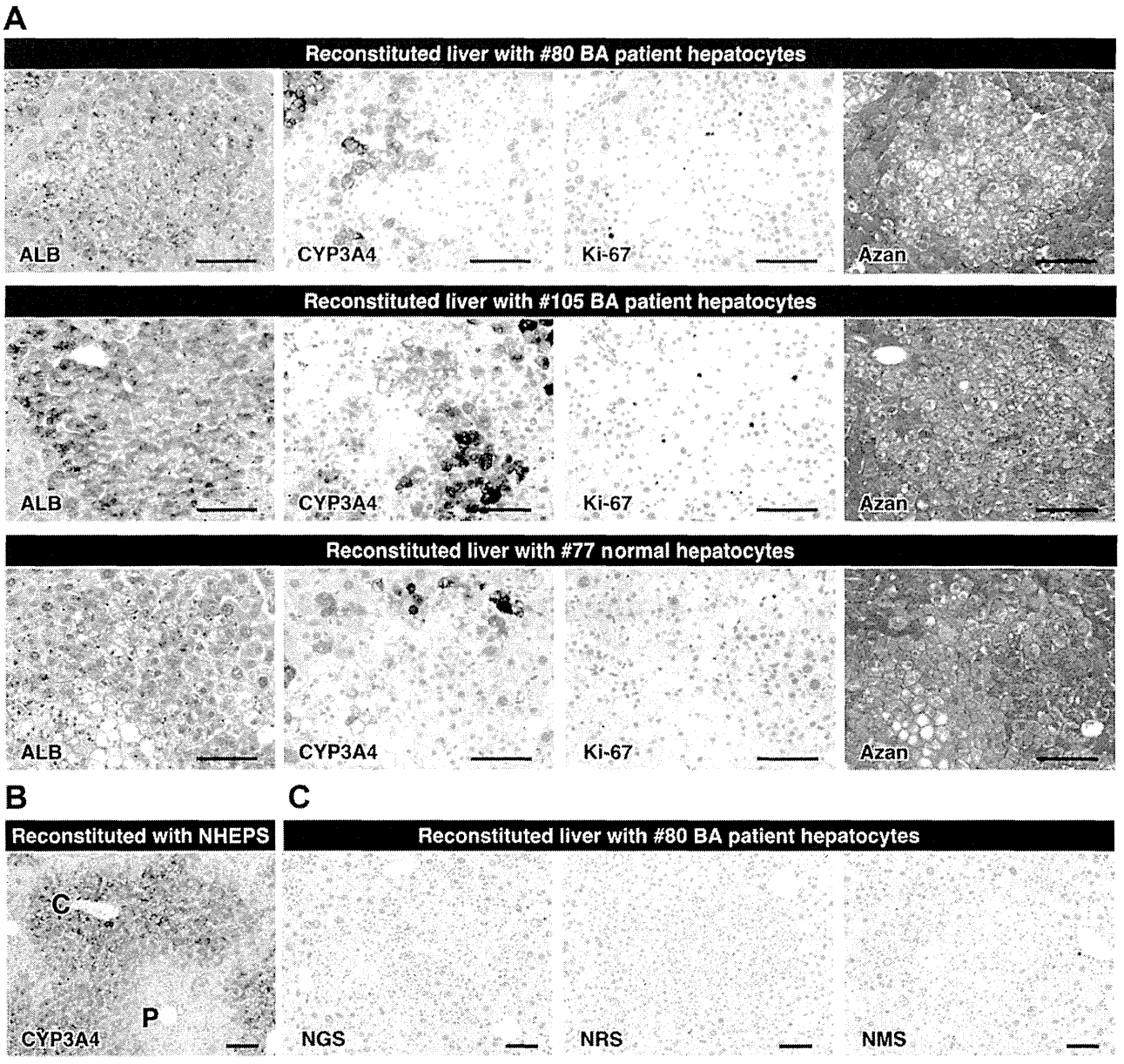

Figure 2. Immunohistochemistry of uPA-NOG mouse livers engrafted with BA patient hepatocytes. (A) Sections were stained for hALB, human CYP3A4, and human Ki-67 antigen; Azan-Mallory staining was also used. The scale bars represent 100 μm. (B) Immunohistochemical staining for CYP3A4 in a fully reconstituted uPA-NOG liver with NHEPS hepatocytes. The scale bar represents 100 μm. (C) Negative controls for immunostaining: NGS, NRS, and NMS. The scale bars represent 100 μm.

process was also observed in the colonies of NHEPS hepatocytes (Fig. 4, middle) but not in the HCT 116 colorectal tumors (Fig. 4, bottom). The typical BC network was detectable in the human hepatocyte conglomerates, as visualized by anti-MRP2, HLA antibodies, and H&E staining (Fig. 4). These results suggest that the intrahepatic bile duct system within the colonies reconstituted with hepatocytes from patients with BA must be nondefective.

DISCUSSION

BA is the most common reason for LT in children worldwide. The aim of this study was to evaluate regenerative medicine as a possible alternative to LT for treating BA. We succeeded in isolating viable hepatocytes from the livers of patients with BA so that we could evaluate the regenerative potential in vivo with a liver failure mouse model.[11] Recently, Gramignoli et al.[28] reported the successful isolation of hepatocytes from people with a number of different metabolic and other liver diseases (n = 35). The purpose of their study was to evaluate hepatocytes from individuals with metabolic disease for use in cell therapy via hepatocyte transplantation. Although they performed hepatocyte isolation in patients with BA (n = 7), those cells would not be recommended for clinical transplants because of concerns about cell yields, viability,

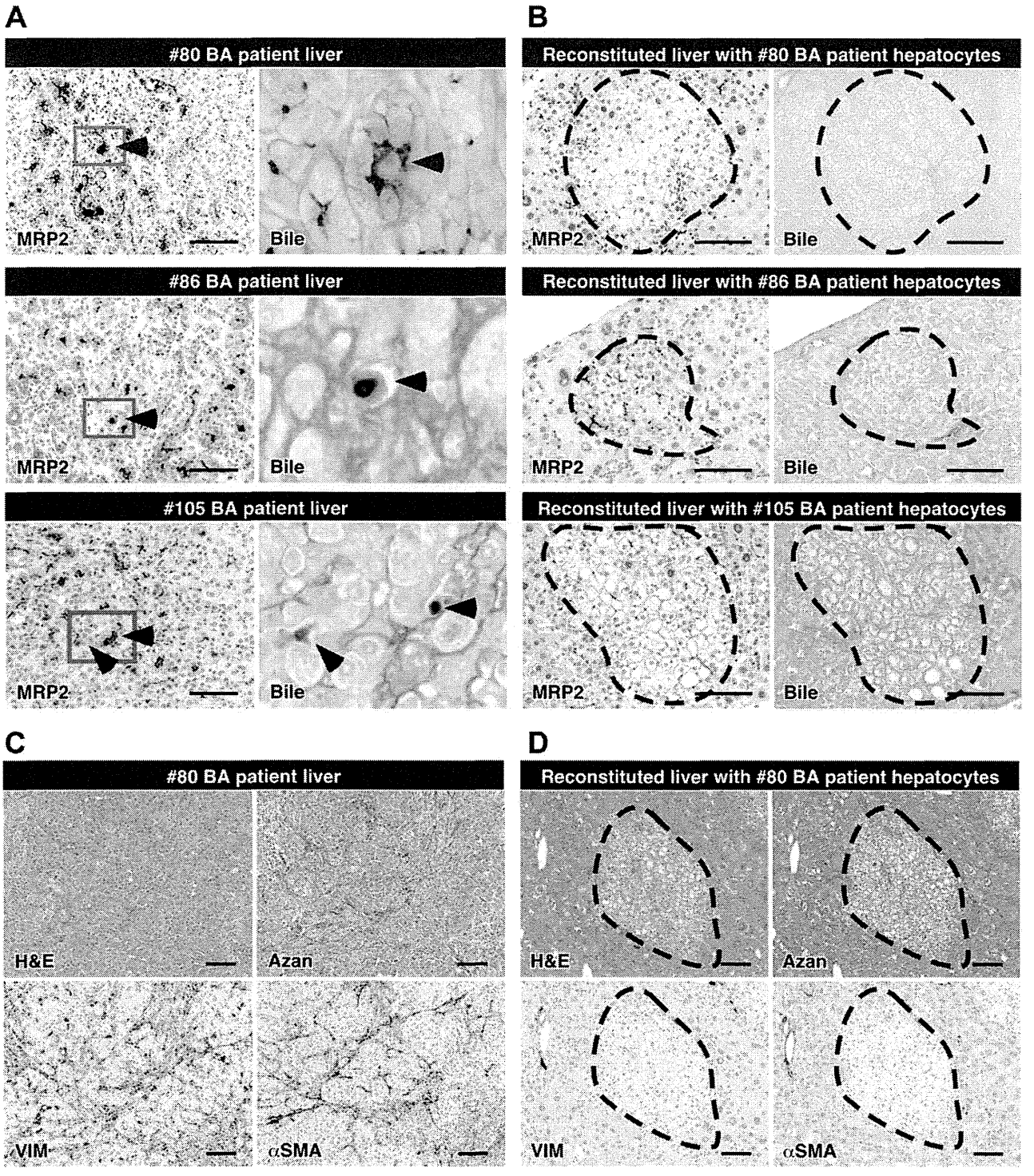

Figure 3. Detection of biliary obstructions and hepatic fibrosis. (A) Immunohistochemical staining for MRP2 protein in livers from patients with BA (patients 80, 86, and 105; left). Enlarged views of the boxed areas are shown with Hall's bilirubin staining (right). Bile stained with Hall's method appears green (arrowheads). (B) Immunohistochemical staining for MRP2 protein (left) and Hall's bilirubin staining (right) in uPA-NOG mouse livers engrafted with hepatocytes from BA patients (patients 80, 86, and 105). The dotted areas indicate the repopulated human liver. (C) H&E and Azan-Mallory staining and immunohistochemical staining for VIM and αSMA in the liver from a BA patient (patient 80). (D) H&E and Azan-Mallory staining and immunohistochemical staining for VIM and αSMA in a uPA-NOG mouse liver engrafted with hepatocytes from a BA patient (patient 80). The dotted areas indicate the repopulated human liver. The scale bars represent 100 μm.

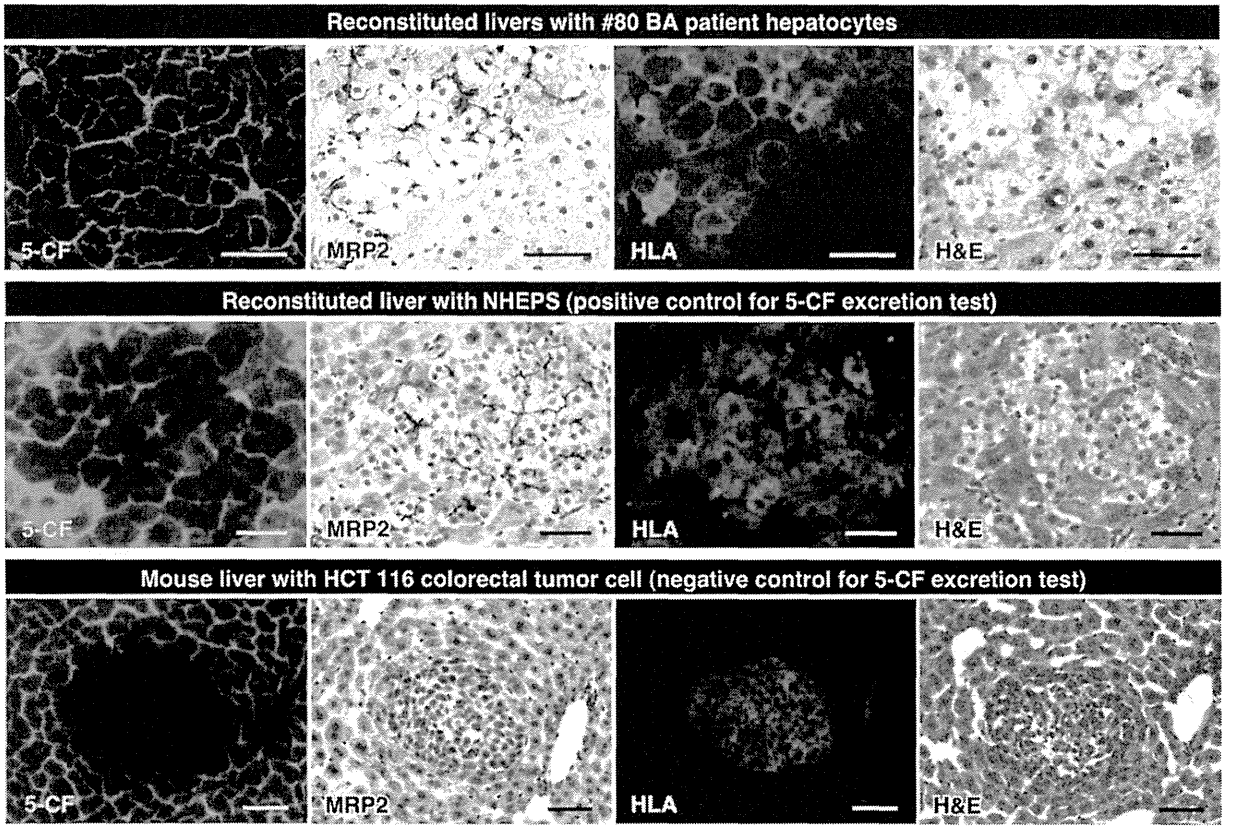

Figure 4. Functional integrity of the BC network within the reconstituted livers. Biliary excretion tests were performed with a fluorescent metabolic marker (5-CFDA). Serial sections were prepared from the livers of mice that received transplants of hepatocytes from a BA patient (patient 80), commercially available cryopreserved hepatocytes (NHEPS; positive control), or HCT 116 colorectal tumor cells (negative control). The sections were loaded with 5-CFDA, and the presence of the fluorescent metabolite 5-CF was assessed. In the livers reconstituted with patient hepatocytes and NHEPS hepatocytes, 5-CF (green on a dark field) was rapidly excreted into the BCs that formed the honeycomb networks over the lobule. In contrast, the BCs around the tumor, which formed after the transplantation of HCT 116 colorectal tumor cells, did not have this honeycomb pattern. Additional sections were stained for human MRP2 (brown in a bright field) and HLA (red in a dark field); H&E staining was also performed. The scale bars represent 50 μm.

and function. Bhogal et al.[29] reported that the viability, the total cell yield, and the success rate with cirrhotic tissues were low. In the current study, the cell yield and cell viability of hepatocytes from BA patients with fibrosis grade II or III were comparable to the yields and viability previously reported by Gramignoli et al. We expected that the low cell yield and viability would depend on the degree of fibrosis in patients with BA. However, there were no significant differences in the cell yields of hepatocytes from patients with grade II fibrosis and hepatocytes from patients with grade III fibrosis (Fig. 1C) or in cell viability (Fig. 1D). These results indicate that regardless of the extent of hepatic fibrosis, the presence of fibrosis affects the cell yield and viability when hepatocytes are isolated from the livers of patients with BA.

For hepatocytes from patient 80, 3 different conditions (freshly isolated, chilled, and frozen-thawed hepatocytes) were compared in terms of their engraftment and proliferative potential in a liver failure model using uPA-NOG mice. HLA-positive hepatocyte colonies were observed in the livers of all uPA-NOG mice that underwent transplantation with hepatocytes of any condition; however, a higher ratio of hALB-secreting mice and a higher level of serum hALB were observed in the mice that underwent transplantation with freshly isolated hepatocytes (Table 2). We succeeded in isolating a small number of hepatocytes buried in the severely cirrhotic liver of BA patient 149 (fibrosis grade III), and surprisingly, the hepatocytes could successfully engraft and proliferate within the uPA-NOG mouse livers as HLA-positive colonies. These results indicate that even hepatocytes buried in the cirrhotic livers of patients with BA do not lose their proliferative potential.

Recent studies of the molecular biology of BA have revealed no significant differences in the hepatic MRP2 expression levels of BA patients and control groups.[30] In fact, we confirmed the expression of not only the adenosine triphosphate–binding cassette, subfamily C (cystic fibrosis transmembrane conductance regulator (CFTR)/multidrug resistance-associated protein (MRP)), member 2 (ABCC2) gene but also the MRP2 protein, which was located on the apical plasma membranes of hepatocytes both in the livers of BA patients (Fig. 3A, left) and in partially humanized livers repopulated with hepatocytes from patients

with BA (Fig. 3B, left). Despite the normal MRP2 protein expression in the livers of patients with BA and in the partially humanized mouse liver, the bile was accumulated only in the many BCs of livers from patients with BA. This result clearly demonstrates the extrahepatic obstruction of the biliary flow.

In this study, using a reconstituted-liver mouse model, we examined the hepatocytes of patients with BA for the presence of abnormalities in vivo. Unfortunately, we failed to establish a BA model with liver-injured mice. However, this result indicates that the primary etiology of BA is absent in the hepatocytes themselves, and the hepatocytes buried in the cirrhotic livers of patients with BA are functionally intact hepatocytes retaining their proliferative potential and able to reconstitute a partially functioning human liver in mice. Gramignoli et al.[28] recently reported the isolation of hepatocytes from patients with many metabolic diseases, including BA, and the rapid and efficient repopulation of FRG (fumarylacetoacetate hydrolase (Fah), recombination activating gene 2 (Rag2) and interleukin 2 receptor gamma chain (Il-2rγ) triple gene knockout) mouse livers after the transplantation of hepatocytes obtained from patients with metabolic disease. In addition to Gramignoli et al.'s report, the current study supports the hypothesis that hepatocytes from patients with BA are morphologically and biochemically normal.

Recently, it has been reported that the extent of liver fibrosis at the time of portoenterostomy, as evaluated by picrosirius red staining, appears to be a strong negative predictor of outcomes.[31] The negative correlation between the extent of liver fibrosis and the yield of viable hepatocytes suggested by our results might be associated with that phenomenon. These results support the possibility that if the primary etiology is removed by Kasai portoenterostomy before progressive cholestasis develops, the liver of the patient with BA may regenerate autologously via the functionally intact hepatocytes remaining in the cirrhotic liver. The hepatocyte function in patients with BA may be independent of the degree of fibrosis; therefore, efforts to ameliorate the fibrosis would have great promise in treating this disease. Treatment would include an earlier diagnosis and surgery but might also include developing antifibrotic pharmacological approaches. If a method for earlier diagnosis or new drugs are developed in the near future, patients with BA may not require an operation that is as difficult as LT.

ACKNOWLEDGMENT

The authors thank M. Kuronuma, Y. Ando, T. Ogura, T. Kamisako, and R. Takahashi for their outstanding technical assistance with the animal experiments. They also thank M. Yamamoto, H. Nabekawa, and C. Kito for their technical assistance with molecular analyses and Dr. M. Ito, S. Enosawa, and M. Onodera for their helpful discussions.

REFERENCES

1. Hartley JL, Davenport M, Kelly DA. Biliary atresia. Lancet 2009;374:1704-1713.
2. Bassett MD, Murray KF. Biliary atresia: recent progress. J Clin Gastroenterol 2008;42:720-729.
3. Muratore CS, Harty MW, Papa EF, Tracy TF Jr. Dexamethasone alters the hepatic inflammatory cellular profile without changes in matrix degradation during liver repair following biliary decompression. J Surg Res 2009; 156:231-239.
4. Sokol RJ, Shepherd RW, Superina R, Bezerra JA, Robuck P, Hoofnagle JH. Screening and outcomes in biliary atresia: summary of a National Institutes of Health workshop. Hepatology 2007;46:566-581.
5. Serinet MO, Wildhaber BE, Broué P, Lachaux A, Sarles J, Jacquemin E, et al. Impact of age at Kasai operation on its results in late childhood and adolescence: a rational basis for biliary atresia screening. Pediatrics 2009;123: 1280-1286.
6. Czech-Schmidt G, Verhagen W, Szavay P, Leonhardt J, Petersen C. Immunological gap in the infectious animal model for biliary atresia. J Surg Res 2001;101:62-67.
7. Petersen C, Biermanns D, Kuske M, Schäkel K, Meyer-Junghänel L, Mildenberger H. New aspects in a murine model for extrahepatic biliary atresia. J Pediatr Surg 1997;32:1190-1195.
8. Riepenhoff-Talty M, Schaekel K, Clark HF, Mueller W, Uhnoo I, Rossi T, et al. Group A rotaviruses produce extrahepatic biliary obstruction in orally inoculated newborn mice. Pediatr Res 1993;33(pt 1):394-399.
9. Dandri M, Burda MR, Török E, Pollok JM, Iwanska A, Sommer G, et al. Repopulation of mouse liver with human hepatocytes and in vivo infection with hepatitis B virus. Hepatology 2001;33:981-988.
10. Mercer DF, Schiller DE, Elliott JF, Douglas DN, Hao C, Rinfret A, et al. Hepatitis C virus replication in mice with chimeric human livers. Nat Med 2001;7:927-933.
11. Suemizu H, Hasegawa M, Kawai K, Taniguchi K, Monnai M, Wakui M, et al. Establishment of a humanized model of liver using NOD/Shi-scid IL2Rgnull mice. Biochem Biophys Res Commun 2008;377:248-252.
12. Barshes NR, Lee TC, Udell IW, O'Mahoney CA, Karpen SJ, Carter BA, Goss JA. The Pediatric End-Stage Liver Disease (PELD) model as a predictor of survival benefit and posttransplant survival in pediatric liver transplant recipients. Liver Transpl 2006;12:475-480.
13. Weerasooriya VS, White FV, Shepherd RW. Hepatic fibrosis and survival in biliary atresia. J Pediatr 2004;144: 123-125.
14. Seglen PO. Preparation of isolated rat liver cells. Methods Cell Biol 1976;13:29-83.
15. Miyamoto Y, Suzuki S, Nomura K, Enosawa S. Improvement of hepatocyte viability after cryopreservation by supplementation of long-chain oligosaccharide in the freezing medium in rats and humans. Cell Transplant 2006;15:911-919.
16. Nakamura K, Mizutani R, Sanbe A, Enosawa S, Kasahara M, Nakagawa A, et al. Evaluation of drug toxicity with hepatocytes cultured in a micro-space cell culture system. J Biosci Bioeng 2011;111:78-84.
17. Hasegawa M, Kawai K, Mitsui T, Taniguchi K, Monnai M, Wakui M, et al. The reconstituted 'humanized liver' in TK-NOG mice is mature and functional. Biochem Biophys Res Commun 2011;405:405-410.
18. Tsukahara T, Kawaguchi S, Torigoe T, Asanuma H, Nakazawa E, Shimozawa K, et al. Prognostic significance of HLA class I expression in osteosarcoma defined by anti-pan HLA class I monoclonal antibody, EMR8-5. Cancer Sci 2006;97:1374-1380.

19. Key G, Becker MH, Baron B, Duchrow M, Schlüter C, Flad HD, Gerdes J. New Ki-67-equivalent murine monoclonal antibodies (MIB 1-3) generated against bacterially expressed parts of the Ki-67 cDNA containing three 62 base pair repetitive elements encoding for the Ki-67 epitope. Lab Invest 1993;68:629-636.
20. Scheffer GL, Kool M, Heijn M, de Haas M, Pijnenborg AC, Wijnholds J, et al. Specific detection of multidrug resistance proteins MRP1, MRP2, MRP3, MRP5, and MDR3 P-glycoprotein with a panel of monoclonal antibodies. Cancer Res 2000;60:5269-5277.
21. Dekel B, Shezen E, Even-Tov-Friedman S, Katchman H, Margalit R, Nagler A, Reisner Y. Transplantation of human hematopoietic stem cells into ischemic and growing kidneys suggests a role in vasculogenesis but not tubulogenesis. Stem Cells 2006;24:1185-1193.
22. Skalli O, Ropraz P, Trzeciak A, Benzonana G, Gillessen D, Gabbiani G. A monoclonal antibody against alpha-smooth muscle actin: a new probe for smooth muscle differentiation. J Cell Biol 1986;103(pt 2):2787-2796.
23. Hall MJ. A staining reaction for bilirubin in sections of tissue. Am J Clin Pathol 1960;34:313-316.
24. Hamada K, Monnai M, Kawai K, Nishime C, Kito C, Miyazaki N, et al. Liver metastasis models of colon cancer for evaluation of drug efficacy using NOD/Shi-scid IL2R-gammanull (NOG) mice. Int J Oncol 2008;32:153-159.
25. Limas C, Bigler A, Bair R, Bernhart P, Reddy P. Proliferative activity of urothelial neoplasms: comparison of BrdU incorporation, Ki67 expression, and nucleolar organiser regions. J Clin Pathol 1993;46:159-165.
26. Mills SJ, Shepherd NA, Hall PA, Hastings A, Mathers JC, Gunn A. Proliferative compartment deregulation in the non-neoplastic colonic epithelium of familial adenomatous polyposis. Gut 1995;36:391-394.
27. Kudo A, Kashiwagi S, Kajimura M, Yoshimura Y, Uchida K, Arii S, Suematsu M. Kupffer cells alter organic anion transport through multidrug resistance protein 2 in the post-cold ischemic rat liver. Hepatology 2004;39:1099-1109.
28. Gramignoli R, Tahan V, Dorko K, Skvorak KJ, Hansel MC, Zhao W, et al. New potential cell source for hepatocyte transplantation: discarded livers from metabolic disease liver transplants. Stem Cell Res 2013;11:563-573.
29. Bhogal RH, Hodson J, Bartlett DC, Weston CJ, Curbishley SM, Haughton E, et al. Isolation of primary human hepatocytes from normal and diseased liver tissue: a one hundred liver experience. PLoS One 2011;6:e18222.
30. Terui K, Saito T, Hishiki T, Sato Y, Mitsunaga T, Yoshida H. Hepatic expression of multidrug resistance protein 2 in biliary atresia. Comp Hepatol 2011;10:6.
31. Pape L, Olsson K, Petersen C, von Wasilewski R, Melter M. Prognostic value of computerized quantification of liver fibrosis in children with biliary atresia. Liver Transpl 2009;15:876-882.

DOI: 10.7589/2013-09-229

Journal of Wildlife Diseases, 50(2), 2014, pp. 412–415

Molecular Evidence for Hemotropic Mycoplasma Infection in a Japanese Badger (*Meles meles anakuma*) and a Raccoon Dog (*Nyctereutes procyonoides viverrinus*)

Ryô Harasawa,[1,4] Riccardo Orusa,[2] and Massimo Giangaspero[3] [1]The Iwate Research Center for Wildlife Diseases, Nakano 1-17-4, Morioka 020-0816, Japan; [2]National Reference Centre for Wild Animal Diseases (CeRMAS), Istituto Zooprofilattico Sperimentale del Piemonte, Liguria e Valle d'Aosta, Via Regione Amerique No. 7/g, 11020 Quart (Aosta), Italy; [3]Faculty of Veterinary Medicine, University of Teramo, Piazza Aldo Moro 45, 64100 Teramo, Italy; [4]Corresponding author (email: harasawa@iwate-u.ac.jp)

ABSTRACT: We report detection of hemoplasma in wild Japanese badgers (*Meles meles anakuma*) and raccoon dogs (*Nyctereutes procyonoides viverrinus*). Sequence analysis of the entire 16S rRNA genes identified *Mycoplasma haemocanis* in the raccoon dog sample, and a potential novel *Mycoplasma* species in the Japanese badger.

Hemoplasma, also referred to as hemotropic mycoplasma, is a newly defined group of uncultivable prokaryotes, which has been recognized as etiologic agents of infectious anemia in mammalian species (Messick 2004). Hemotropic mycoplasma have been primarily classified through the use of nucleotide sequences of the 16S rRNA gene due to a lack of an appropriate means by which examine its biologic or serologic properties (Messick 2004). Hemoplasmas have been found in several wild animals, including black howler monkeys (*Alouatta caraya*) and reindeer (*Rangifer tarandus*; Stoffregen et al. 2006; Santos et al. 2013), but never previously in Japanese badgers (*Meles meles anakuma*) or raccoon dogs (*Nyctereutes procyonoides viverrinus*). We screened necropsy samples from a Japanese badger and a raccoon dog for hemotropic mycoplasmas by PCR. Here we report hemoplasma detection in these wild animals and a novel hemoplasma in Japanese badgers based on analysis of the 16S rRNA gene.

A young female raccoon dog was found on 12 April 2013 in a barn (39°01′03″N, 141°03′04″E) in Morioka. The body and skull exhibited severe injuries, probably due to attack by other animals. An adult female Japanese badger was found on 17 April 2013 on a road (39°01′02″N, 141°02′06″E) in Morioka. It exhibited traumatic injuries on the abdomen and both legs, probably as a result of a traffic accident. Both animals were brought to a wildlife shelter for rescue but died before emergency treatment. They were subjected to autopsy without clinical examination, and biologic samples were collected for research. Ethylenediaminetetraacetic acid-anticoagulated blood samples were collected from the hearts of both animals and stored at −20 C until examination.

Total DNA was extracted from 200 µL blood samples collected from both animals using the QIAamp DNA Blood Mini Kit (Qiagen, Hilden, Germany) according to the manufacturer's instructions. Negative controls consisting of 200 µL phosphate-buffered saline solutions were prepared with each batch. Extracted DNA samples

TABLE 1. PCR primers described in the text. Primer sequences and positions were derived from the 16S rRNA gene sequence of *Mycoplasma wenyonii* (accession AY946266).

Primer name	Sequence (5′–3′)	Position	Product (bp)
Hemo-F1	5′-AGAGTTTGATCCTGGCTCAG-3′	11–30	
Hemo-R1	5′-TACCTTGTTACGACTTAACT-3′	503–522	512
Hemo-F2	5′-ATATTCCTACGGGAAGCAGC-3′	328–347	
Hemo-R2	5′-ACCGCAGCTGCTGGCACATA-3′	1,446–1,465	1,138

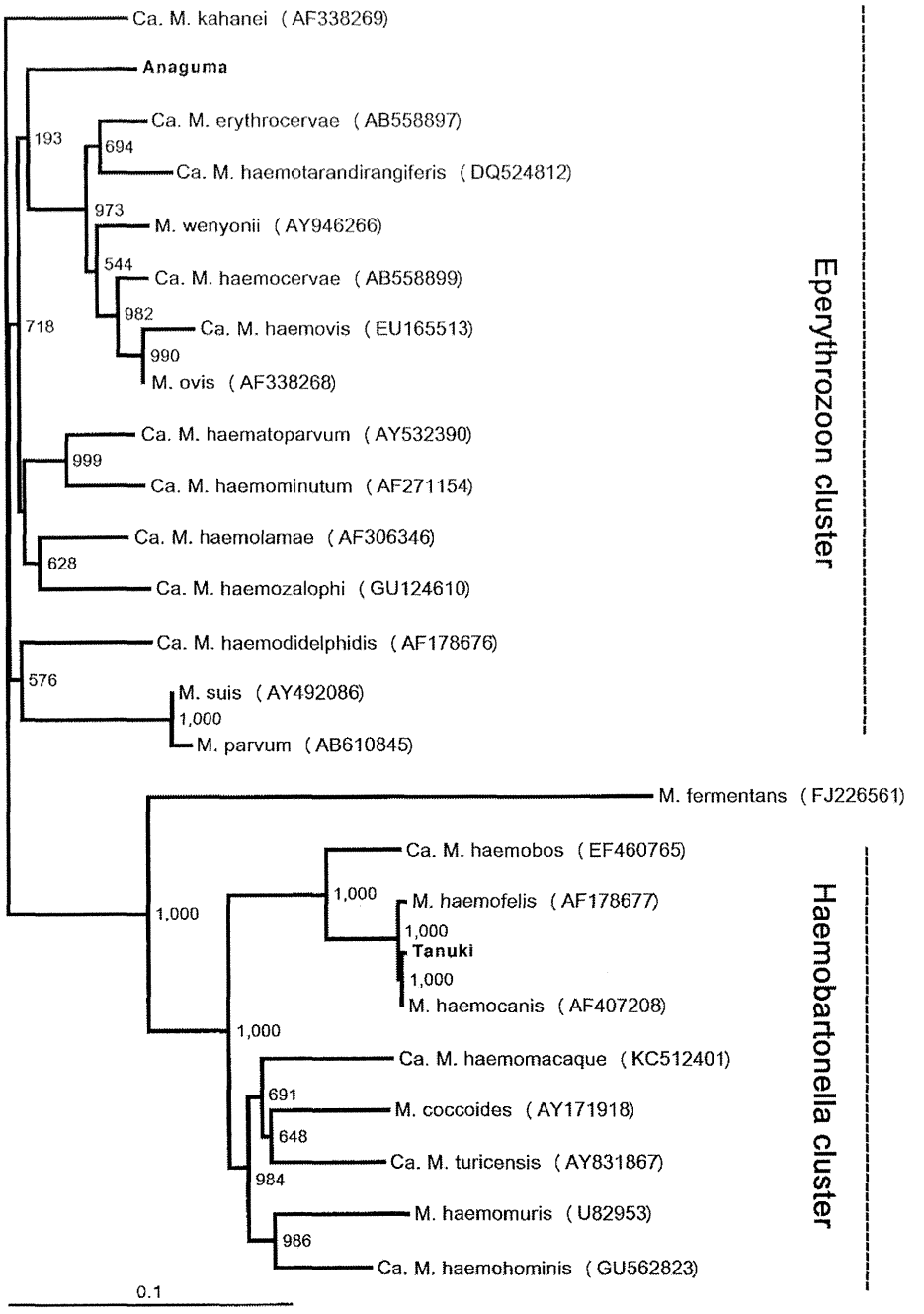

FIGURE 1. A neighbor-joining phylogenetic tree based on a 16S rRNA gene comparison among *Mycoplasma* strains (accession numbers are given in parentheses) which includes the Tanuki strain of *M. haemocanis* and a putative taxon created by the Anaguma strain, despite a low bootstrap value. A classical *Mycoplasma* species, *M. fermentans*, was included as an outgroup. Numbers at the branch points refer to the values of bootstrap probability of 1,000 replications. The tree is drawn to scale, with branch lengths employing the same units as those of the evolutionary distances that were used to infer the phylogenetic tree (scale bar, 0.1 nucleotide substitutions per site).

were subjected to concentration measurements in a GeneQuant II spectrophotometer (GE Healthcare, Tokyo, Japan) and stored at −20 C prior to examination.

For preliminary hemoplasma infection screening, specific PCR primers Hemo-F2 and Hemo-R2 for the 16S rRNA gene (Table 1) were used in the real-time PCR assay with 100 copies sensitivity as described previously (Nishizawa et al. 2010). No signal was evident in the negative controls. End-point PCR was carried out with forward primer Hemo-F1 or Hemo-F2 and reverse primer Hemo-R1 or Hemo-R2 as described previously (Nishizawa et al. 2010). To avoid contamination, PCR and agarose gel electrophoresis were performed in a separate room.

Sequences of 1,425 base pair (bp) from each animal, designated as Tanuki (raccoon dog) and Anaguma (Japanese badger), and deposited in DNA databases under the accession numbers AB848714 and AB848713, were aligned and compared with 23 *Mycoplasma* sequences.

The nucleotide sequence of the 16S rRNA gene has been widely used for identifying uncultivable microorganisms as new species. Hemoplasmas are divided into two phylogenetic clusters corresponding to the formerly *Haemobartonella* and *Eperythrozoon* genera, which have been characterized by 25-bp deletion in the 16S rRNA gene sequence of the *Haemobartonella* genus (Neimark et al. 2004).

The phylogenetic tree (Fig. 1) for the 16S rRNA gene constructed by the algorithms in the PHYLIP program (DDBJ, Mishima, Japan) using the neighbor-joining method (Saitou and Nei 1987) indicated that the hemoplasma strain (1,425 bp) detected in the raccoon dog was located in the Haemobartonella cluster and closely related to a canine hemoplasma, *Mycoplasma haemocanis* (1,393 bp), with a 99% similarity, which is higher than the cut-off level for species differentiation (Drancourt and Raoult 2005). This might be due to a close genealogical relationship between the host animals, which are both in the *Canidae*.

The 16S rRNA gene sequence (1,425 bp) from the Anaguma strain detected in the Japanese badger was more closely related to '*Candidatus* M. erythrocervae' (1,434 bp), '*Ca.* M. haemotarandirangiferis' (651 bp), *M. wenyonii* (1,465 bp), '*Ca.* M. haemovis' (1,441 bp), and *M. ovis* (1,458 bp) in the Eperythrozoon cluster, but with only 91%, 90%, 91%, 87%, and 90% identity, respectively, suggesting a novel hemoplasma species.

Although classical mycoplasmas, including ureaplasmas, have been demonstrated in Japanese badgers and raccoon dogs (Kanamoto et al. 1981, 1983), hemotropic mycoplasmas have never been documented in these species, either free-ranging or captive. This study is the first to reveal a *M. haemocanis* infection in a raccoon dog as well as a previously unknown hemoplasma species in a Japanese badger. We tentatively named this new species '*Candidatus* M. haemomeles,' although its pathogenic traits remained unexplored.

We thank S. Tsunokake and S. Inohana for their help in collecting the samples at the Iwate Wildlife Conservation Center, Takizawa, Japan.

LITERATURE CITED

Drancourt M, Raoult D. 2005. Sequence-based identification of new bacteria: A proposition for creation of an orphan bacterium repository. *J Clin Microbiol* 43:4311–4315.

Kanamoto Y, Kotani H, Ogata M, Fukumoto Y. 1981. Isolation of mycoplasmas from raccoon dog (*Nyctereutes procyonoides viverrinus*), fox (*Vulpes vulpes japonica*) and Japanese badger (*Meles meles anakuma*). *Jpn J Vet Sci* 43:267–271.

Kanamoto Y, Kotani H, Ogata M, Matsuo Y. 1983. Isolation of *Mycoplasma* and *Ureaplasma* species from raccoon dogs (*Nyctereutes procyonoides viverrinus*). *J Gen Microbiol* 129:2447–2450.

Messick JB. 2004. Hemotrophic mycoplasmas (hemoplasmas): A review and new insights into pathogenic potential. *Vet Clin Pathol* 33:2–13.

Neimark H, Hoff B, Ganter M. 2004. *Mycoplasma ovis* comb. nov. (formerly *Eperythrozoon ovis*), an epierythrocytic agent of haemolytic anaemia in sheep and goats. *Int J Syst Evol Microbiol* 54:365–371.

Nishizawa I, Sato M, Fujihara M, Sato S, Harasawa R. 2010. Differential detection of hemotropic *Mycoplasma* species in cattle by melting curve analysis of PCR products. *J Vet Med Sci* 72:77–79. (Erratum, *J Vet Med Sci* 72:1704.)

Saitou N, Nei M. 1987. The neighbor-joining method: A new method for reconstructing phylogenetic trees. *Mol Biol Evol* 4:406–425.

Santos LC, Cubilla MP, de Moraes W, Cubas ZS, Oliveira MJ, Estrada M, Leutenegger CM, Sykes JE, Lindsay LL, Marcondes M, et al. 2013. Hemotropic mycoplasma in a free-ranging black howler monkey (*Alouatta caraya*) in Brazil. *J Wildl Dis* 49:728–731.

Stoffregen WC, Alt DP, Palmer MV, Olse SC, Waters WR, Stasko JA. 2006. Identification of a haemomycoplasma species in anemic reindeer (*Rangifer tarndus*). *J Wildl Dis* 42:249–258.

Submitted for publication 3 September 2013.
Accepted 25 October 2013.

NOTE *Wildlife Science*

Molecular Demonstration of Hemotropic Mycoplasmas in Wild Japanese Monkeys (*Macaca fuscata*)

Hinako SASHIDA[1, 2], Yoshihisa SUZUKI[3], Sou ROKUHARA[3], Kazuya NAGAI[4] and Ryô HARASAWA[2]*

[1]*Department of Veterinary Medicine, Faculty of Agriculture, Iwate University, Morioka 020–8550, Japan*
[2]*The Iwate Research Center for Wildlife Diseases, Morioka 020–0816, Japan*
[3]*The Sarudokonet, NPO for Wildlife Management, Matsusaka 519–2144, Japan*
[4]*Cryobiofrontier Research Center, Faculty of Agriculture, Iwate University, Morioka 020–8550, Japan*

(Received 26 June 2013/Accepted 12 August 2013/Published online in J-STAGE 26 August 2013)

ABSTRACT. The prevalence of hemotropic mycoplasmas in wild monkeys is largely unknown. Here we report the presence of hemoplasmas in blood specimens collected from wild Japanese monkeys (*Macaca fuscata*) tentatively captured for ecological survey in Mie prefecture, Japan. We examined 9 monkeys using hemoplasma-specific real-time PCR and found all of them positive for a hemoplasma infection. The 16S rRNA gene and 16S to 23S rRNA intergenic spacer region of the hemoplasma detected in wild monkeys were amplified using end-point PCR. The nucleotide sequences of the PCR products were further determined and compared to those of other hemoplasmas. Our examinations revealed a wide prevalence of a hemoplasma strain in Japanese monkeys, which was similar to '*Candidatus* Mycoplasma haemomacaque' reported in cynomolgus monkeys (*Macaca fascicularis*). Pathogenic traits of this hemoplasma strain remain unexplored.
KEY WORDS: hemoplasma, monkey, mycoplasma.

doi: 10.1292/jvms.13-0332; *J. Vet. Med. Sci.* 76(1): 97–101, 2014

Hemotropic mycoplasma, also called hemoplasma, is a newly defined group of uncultivable pathogens, which has been classified solely using nucleotide sequences of the 16S rRNA or RNase P RNA genes. Hemotropic mycoplasma has been identified and classified in this manner, because of a lack of an appropriate means to examine its biological or serological property [14]. This group is composed of formerly *Eperythrozoon* and *Hemobartonella*(previously *Bartonella*) species and newly identified hemotropic mycoplasmas. Hemoplasma infection, which is accompanied by erythrocyte hemolysis, has been reported in a variety of mammalian species [14]. Hemoplasmas have been detected in some primates including squirrel monkeys (*Saimiri sciureus*), owl monkeys (*Aotus trivirgatus*), rhesus monkeys (*Macaca mulatta*), cynomolgus monkeys (*Macaca fascicularis*) and humans (*Homo sapiens*) as an etiological agent of infectious anemia [1, 3, 18, 22]. Provisional hemoplasma species in primates have been proposed as '*Candidatus* Mycoplasma kahanei' in squirrel monkeys [17], '*Ca.* M. aoti' in owl monkeys [2], '*Ca.* M. haemomacaque' in cynomolgus monkeys [13] and '*Ca.* M. haemohominis' in humans [20]. However, the prevalence of hemoplasma infections in Japanese monkeys (*Macaca fuscata*) that live throughout Japan has remained largely unknown. In this report, we demonstrate a hemoplasma strain in Japanese monkeys that is similar to '*Ca.* M. haemomacaque' reported in the U.S.A.

Ethylenediaminetetraacetic acid (EDTA)-anticoagulated blood samples were collected by saphenous venipuncture from nine wild Japanese monkeys under anesthesia with Zoletil (Virbac, Peakhurst, NSW, Australia) in accordance with the Guidelines for Care and Use of Laboratory Animals of our institutions and stored at −80°C prior to examination. The blood samples were taken for ecological research purpose in Mie prefecture, Japan between October 2012 and February 2013, and the reminder was used for this study. All the monkeys, tentatively captured and released, were apparently healthy, and their age upon capture was unknown. No hematologic parameters were recorded in this study. Total DNA was extracted from 200 μl blood samples collected from Japanese monkeys using the QIAamp DNA Blood Mini Kit (Qiagen, Hilden, Germany) according to the manufacturer's instructions. Negative controls consisting of 200 μl phosphate-buffered saline solution were prepared with each batch. Extracted DNA samples were stored at −80°C prior to examination.

For preliminary screening of hemoplasma infection, specific PCR primers (forward primer: 5′-ATATTCCTACGGGAAGCAGC-3′ equivalent to nucleotide numbers 328 to 347 of *M. wenyonii* [AY946266] and reverse primer: 5′-ACCGCAGCTGCTGGCACATA-3′ equivalent to nucleotide numbers 503 to 522 of *M. wenyonii*) for the 16S rRNA gene of hemoplasmas were used in real-time PCR assay. Real-time PCR was performed in a SmartCycler instrument (Cepheid, Sunnyvale, CA, U.S.A.) with SYBR Premix Ex *Taq*(TaKaRa Bio., Otsu, Japan) as described previously [11]. Of the nine blood samples tested using real-time PCR, all the monkeys were found to be positive for a hemoplasma infection. No signal was evident in negative controls.

After real-time PCR, the melting experiment was per-

* CORRESPONDENCE TO: HARASAWA, R, The Iwate Research Center for Wildlife Diseases, Morioka 020–0816, Japan.
e-mail: harasawa-tky@umin.ac.jp

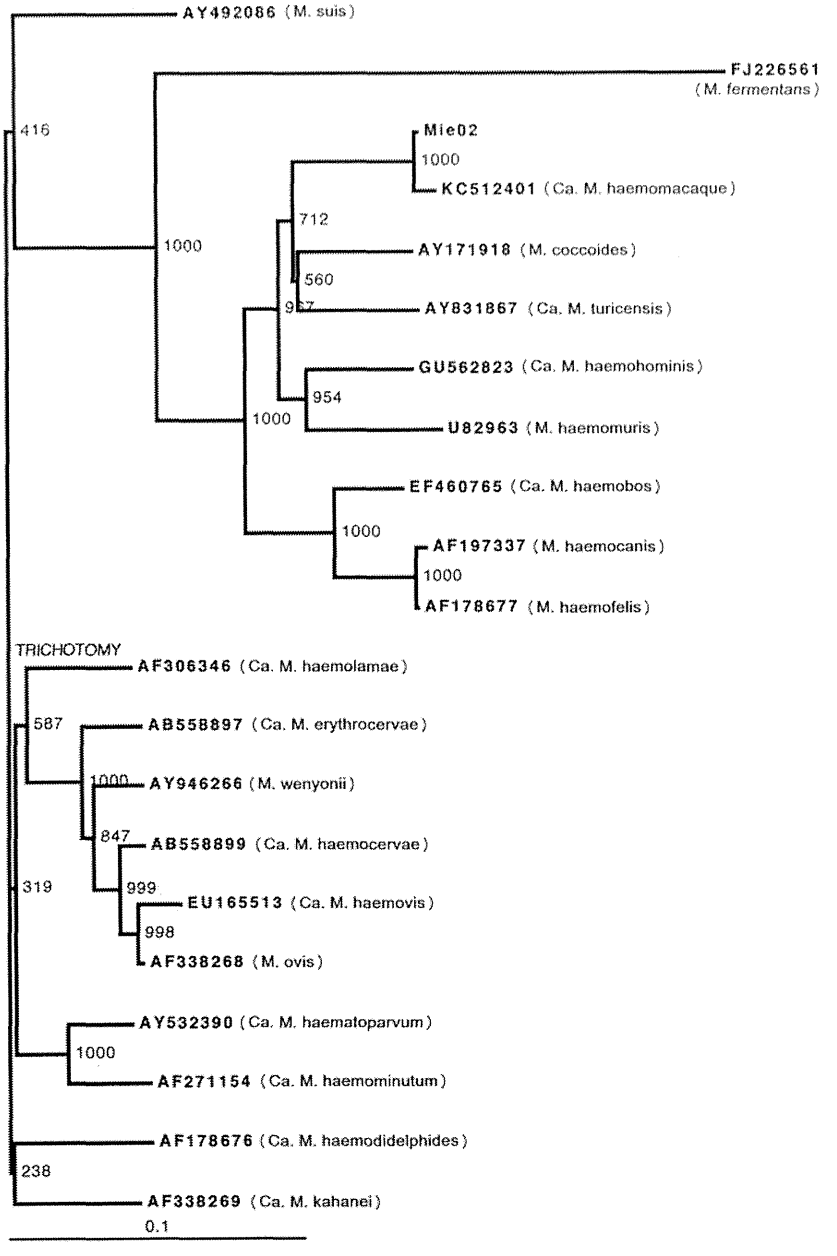

Fig. 1. Comprehensive neighbor-joining phylogenetic tree generated by the nucleotide sequences of 16S rRNA genes showing the evolutionary relationship among 20 established *Mycoplasma* species and a hemoplasma strain Mie02 detected in a Japanese monkey. *Mycoplasma fermentans* PG18 (FJ226561) was included as an out-group. The bootstrap values are indicated at the branch points. The tree is drawn to scale with branch lengths in the same units as those of the evolutionary distances that were used to infer the phylogenetic tree (scale bar, 0.1 nucleotide substitutions per site).

formed as described previously [10]. The melting temperature (*Tm*) of the positive sample was depicted as a single peak at about 84.5°C (data not shown), suggesting a specific amplification. This *Tm* value, higher than those of bear hemoplasmas [11], seemed peculiar to this hemoplasma strain and useful for a differential marker of species identification as described elsewhere [10]. Our previous experiments indicated that the input amount of DNA, the copy number of the target and the presence of co-infections with several targets did not influence the *Tm* [10].

The nine positive samples in the real-time PCR experiment were further subjected to end-point PCR to amplify

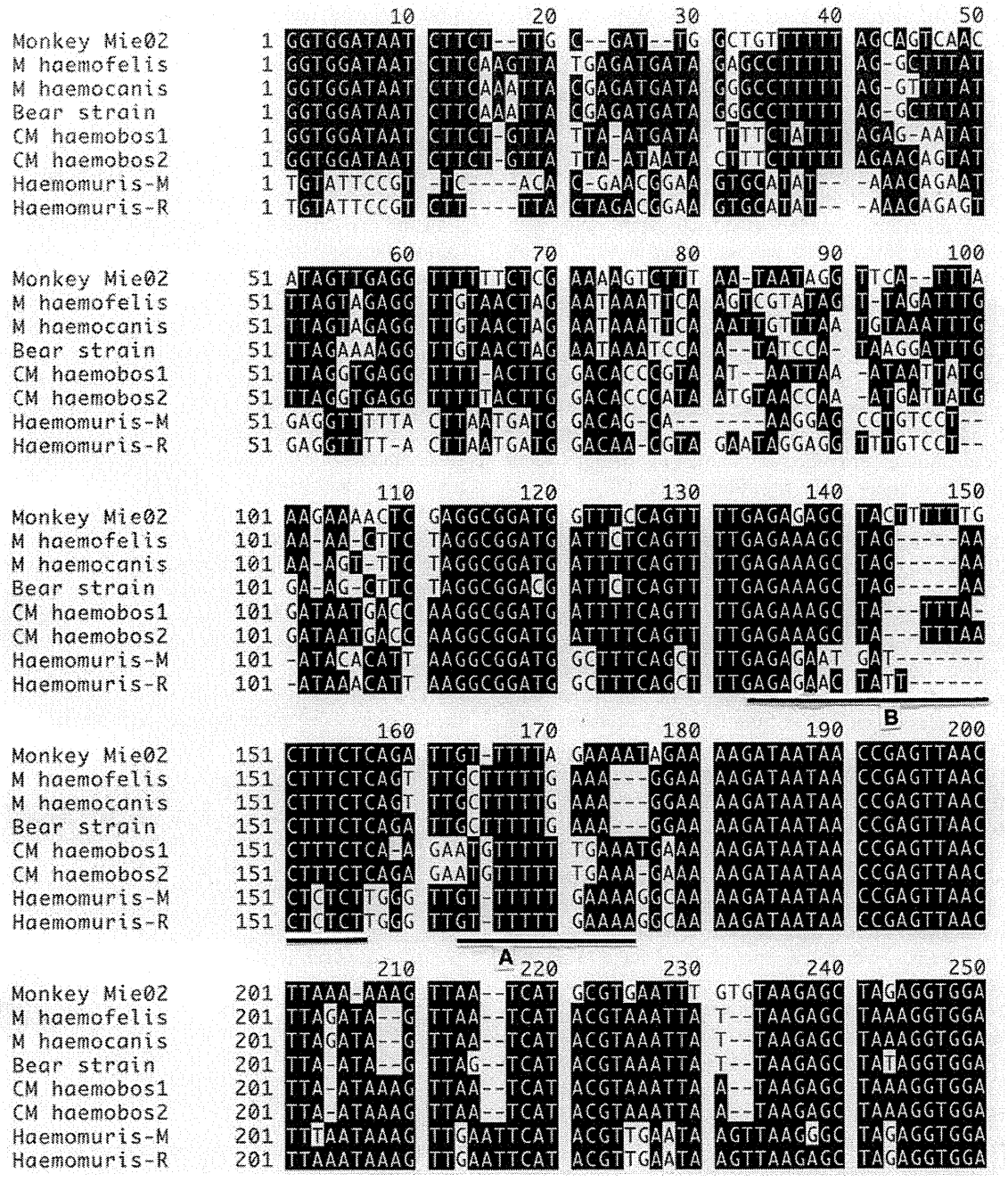

Fig. 2. Nucleotide sequence alignment of the ITS region from the seven hemoplasma sequences, (*M. haemofelis*, *M. haemocanis*, '*Candidatus* M. haemobos' types 1 and 2, *M. haemomuris* subsp. *musculi*(Haemomuris-M) and *M. haemomuris* subsp. *ratti*(Haemomuris-R), bear strain [11] and the Mie02 monkey strain. Accession numbers for the nucleotide sequences of *M. haemomuris* subsp. *musculi, M. haemomuris* subsp. *ratti, M. haemofelis, M. haemocanis, 'Ca.* M. haemobos' types 1 and 2, and bear strain are AB080799, AB758434, AB638408, AF197337, AB638407, AB740010 and AB725596, respectively. Nucleotide sequence numbers are given from a consensus sequence. Homologous nucleotides are shown as inverted characters. Dashes indicate nucleotide gaps between adjacent nucleotides introduced for the alignment. BoxA and boxB are underlined as A and B, respectively.

the entire region of the 16S rRNA gene. End-point PCR was carried out with 50-μl reaction mixtures each containing 1 μl of DNA solution, 0.8 μl of Tks Gflex DNA polymerase (1.25 units/μl), 25 μl of 2X Gflex PCR buffer (TaKaRa Bio.), 0.2 μl each of the forward primer (5′-AGAGTTT-GATCCTGGCTCAG-3′, equivalent to nucleotide numbers

11 to 30 of *M. wenyonii*(AY946266) or 5′- ATATTCCTAC-GGGAAGCAGC-3′, which is equivalent to nucleotide numbers 328 to 347 of *M. wenyonii*) and the reverse primer (5′- ACCGCAGCTGCTGGCACATA-3′, equivalent to nucleotide numbers 503 to 522 of *M. wenyonii* or 5′-TACCTT-GTTACGACTTAACT-3′, equivalent to nucleotide numbers 1446 to 1465 of *M. wenyonii*) (50 pmol/μl each) and water to a final volume of 50 μl. After initial denaturation at 94°C for 5 min, the reaction cycle was carried out 30 times with denaturation at 98°C for 10 sec, annealing at 60°C for 60 sec, extension at 68°C for 30 sec and final extention at 68°C for 5 min in a thermal cycler. The end-point PCR product from the 16S rRNA gene was fractionated on horizontal, submerged 1.0% SeaKem ME agarose gels (FMC Bioproducts, Rockland, ME, U.S.A.) in TAE buffer (40 mM Tris, pH8.0, 5 mM sodium acetate, and 1 mM disodium EDTA) at 100 volts for 30 min. After electrophoresis, the gels were stained in ethidium bromide solution (0.4 μg/m*l*) for 15 min and visualized under a UV transilluminator. DNA was extracted using a NucleoSpin Extract II kit (Macherey-Nagel, Düren, Germany) and was subjected to direct sequencing in a 3500 Genetic Analyzer (Applied Biosystems, Foster City, CA, U.S.A.).

The nucleotide sequences of 16S rRNA gene in hemoplasmas from the nine Japanese monkeys were identical each other. The 16S rRNA gene sequence obtained from hemoplasmas in Japanese monkeys was compared with other hemoplasma sequences from the DNA database using Clustal W [21]. A phylogenetic tree was generated using the neighbor-joining method [19] from a distance matrix corrected for nucleotide substitutions using the Kimura 2-parameter model [12]. The data were re-sampled 1,000 times to generate bootstrap values (Fig. 1). The 16S rRNA gene nucleotide sequence of hemoplasma strain Mie02 detected in a Japanese monkey was most closely related to '*Ca.* M. haemomacaque' in the tree. Sequence similarity between them was 97.9%, which was enough level for a same species [4]. '*Ca.* M. haemomacaque' was first reported in the blood of cynomolgus monkeys in a research colony by assessing the 16S rRNA and RNase P RNA genes [13]. The 16S rRNA gene sequences are widely used in microbiology for identifying uncultivable microorganisms as new species; 16S rRNA gene sequences have also been the basis for the reclassification of hemotropic *Mycoplasma* species [15, 16]. We tried to amplify the RNase P RNA gene using PCR, but only to fail.

Subsequently, we amplified the 16S-23S rRNA intergenic transcribed spacer (ITS) region of the hemoplasmas detected in Japanese monkeys using end-point PCR with the forward primer (5′-GTTCCCAGGTCTTGTACACA-3′) and the reverse primer (5′-CAGTACTTGTTCACTGGTA-3′) as described previously [8]. Reaction was the same as used for the amplification of the 16S rRNA gene, except for the annealing temperature at 55°C instead of 60°C and the extention time for 15 sec instead of 30 sec. The ITS region nucleotide sequence of strain Mie02 was determined as described above and compared to those of other hemoplasmas (Fig. 2). The ITS region of the genus *Mycoplasma* is well conserved within a species and has been used for a genetic marker for identification and classification of mycoplasmas [5]. No spacer tRNA gene was identified within the ITS region of this hemoplasma strain, which is a common feature that is consistent with the other species of the genus *Mycoplasma* [6, 7]. The hemoplasma strain detected in Japanese monkeys possessed the boxA and boxB motifs that are common to other mycoplasma species examined so far [9].

In the present study, we detected hemoplasmas in nine captive Japanese monkeys, which shared a same nucleotide sequence of the 16S rRNA gene and ITS region, suggesting that the same strain was circulating among Japanese monkeys in Mie prefecture, Japan. We then used 16S rRNA phylogenetic analysis to demonstrate the hemoplasma strain that was most closely related to '*Ca.* M. haemomacaque' recently reported in the U.S.A. [13]. The incidence of hemoplasma infection in Japanese monkeys was 100% (9/9), despite a small number of examinations, whereas 84.6% (44/52) in cynomolgus monkeys in the U.S.A. [13]. Although we awaited our identification as '*Ca.* M. haemomacaque' until examination of the RNase P RNA gene, our results suggested a wide prevalence of the hemoplasma strain similar to '*Ca.* M. haemomacaque' in wild Japanese monkeys. It is particularly of interest that the genetically related hemoplasma strains were observed in geographically separate populations. The nucleotide sequence of the 16S rRNA gene combined with the ITS region of the monkey strain has been deposited to the DNA database under the accession number AB820288.

REFERENCES

1. Aikawa, M. and Nussenzwig, R. 1972. Fine structure of *Haemobartonella* sp. in the squirrel monkey. *J. Parasitol.* **58**: 628–630. [CrossRef] [Medline]
2. Barker, E. N., Helps, C. R., Neimark, H., Peters, I. R., Peters, W. and Tasker, S. 2011. A novel haemoplasma species identified in archived primate blood smears. *Vet. Microbiol.* **149**: 478–481. [CrossRef] [Medline]
3. Dillberger, J. E., Loudy, D. E., Adler, R. R. and Gass, J. H. 1994. Haemobartonella-like parasites in cynomolgus monkeys. *Vet. Pathol.* **31**: 301–307. [CrossRef] [Medline]
4. Drancourt, M. and Raoult, D. 2005. Sequence-based identification of new bacteria: a proposition for creation of an orphan bacterium repository. *J. Clin. Microbiol.* **43**: 4311–4315. [CrossRef] [Medline]
5. Harasawa, R. 1999. Genetic relationships among mycoplasmas based on the 16S-23S rRNA spacer sequence. *Microbiol. Immunol.* **43**: 127–132. [Medline]
6. Harasawa, R., Hotzel, H. and Sachse, K. 2000. Comparison of the 16S-23S rRNA intergenic spacer regions among strains of the *Mycoplasma mycoides* cluster, and reassessment of the taxonomic position of *Mycoplasma* sp. bovine group 7. *Int. J. Syst. Evol. Microbiol.* **50**: 1325–1329. [CrossRef] [Medline]
7. Harasawa, R., Pitcher, D. G., Ramirez, A. S. and Bradbury, J. M. 2004. A putative transposase gene in the 16S-23S rRNA intergenic spacer region of *Mycoplasma imitans*. *Microbiology* **150**: 1023–1029. [CrossRef] [Medline]
8. Harasawa, R., Uemori, T., Asada, K. and Kato, I. 1993. Sensitive detection of mycoplasmas in cell cultures by using two-step polymerase chain reaction. pp. 227–232. *In*: Rapid Diagnosis of

Mycoplasmas (Kahane, I. and Adoni, A. eds.), Plenum Press, New York.
9. Harasawa, R., Uemori, T., Asada, K., Kato, I. and Shiragami, N. 1992. 'boxA'-like sequence between the 16S/23S spacer in the rRNA operon. *FEBS Lett.* **297**: 209–211. [CrossRef] [Medline]
10. Harasawa, R., Mizusawa, H., Fujii, M., Yamamoto, J., Mukai, H., Uemori, T., Asada, K. and Kato, I. 2005. Rapid detection and differentiation of the major mycoplasma contaminants in cell cultures using real-time PCR with SYBR Green I and melting curve analysis. *Microbiol. Immunol.* **49**: 859–863. [Medline]
11. Iso, T., Suzuki, J., Sasaoka, F., Sashida, H., Watanabe, Y., Fujihara, N., Nagai, K. and Harasawa, R. 2013. Hemotropic mycoplasma infection in wild black bears (*Ursus thibetanus japonicus*). *Vet. Microbiol.* **163**: 184–189. [CrossRef] [Medline]
12. Kimura, M. 1980. A simple method for estimating evolutionary rates of base substitutions through comparative studies of nucleotide sequences. *J. Mol. Evol.* **16**: 111–120. [CrossRef] [Medline]
13. Maggi, R. G., Mascarelli, P. E., Balakrishnan, N., Rohde, C. M., Kelly, C. M., Ramaiah, L., Leach, M. W. and Breitschwerdt, E. B. 2013. '*Candidatus* Mycoplasma haemomacaque' and *Bartonella quintana* bacteremia in cynomolgus monkeys. *J. Clin. Microbiol.* **51**: 1408–1411 [CrossRef]. [Medline]
14. Messick, J. B. 2004. Hemotrophic mycoplasmas (hemoplasmas): a review and new insights into pathogenic potential. *Vet. Clin. Pathol.* **33**: 2–13. [CrossRef] [Medline]
15. Neimark, H., Johansson, K.E., Rikihisa, Y. and Tully, J. G. 2001. Proposal to transfer some members of the genera *Haemobartonella* and *Eperythrozoon* to the genus *Mycoplasma* with descriptions of '*Candidatus* Mycoplasma haemofelis', '*Candidatus* Mycoplasma haemomuris', '*Candidatus* Mycoplasma haemosuis' and '*Candidatus* Mycoplasma wenyonii'. *Int. J. Syst. Evol. Microbiol.* **51**: 891–899. [CrossRef] [Medline]
16. Neimark, H., Johansson, K.E., Rikihisa, Y. and Tully, J. G. 2002. Revision of haemotrophic mycoplasma species names. *Int. J. Syst. Evol. Microbiol.* **52**: 683. [Medline]
17. Neimark, H., Barnaud, A., Gounon, P., Miche, J.C. and Contamin, H. 2002. The putative haemobartonella that influences *Plasmodium falciparum* parasitaemia in squirrel monkeys is a haemotropic mycoplasma. *Microb. Infect.* **4**: 693–698. [CrossRef]
18. Peters, W., Molyneux, D. H. and Howells, R. E. 1974. *Eperythrozoon* and *Haemobartonella* in monkeys. *Ann. Trop. Med. Parasitol.* **68**: 47–50. [Medline]
19. Saitou, N. and Nei, M. 1987. The neighbor-joining method: a new method for reconstructing phylogenetic trees. *Mol. Biol. Evol.* **4**: 406–425. [Medline]
20. Steer, J. A., Tasker, S., Barker, E. N., Jensen, J., Mitchell, J., Stocki, T., Chalker, V. J. and Hamon, M. 2011. A novel hemotropic mycoplasma (hemoplasma) in a patient with hemolytic anemia and pyrexia. *Clin. Infect. Dis.* **53**: e147–e151. [CrossRef] [Medline]
21. Thompson, J. D., Higgins, D. G. and Gibson, T. J. 1994. CLUSTAL W: improving the sensitivity of progressive multiple sequence alignment through sequence weighting, position-specific gap penalties and weight matrix choice. *Nucleic Acids Res.* **22**: 4673–4680. [CrossRef] [Medline]
22. Yuan, C., Liang, A., Yu, F., Yang, Z., Li, Z., Zhu, J., Cui, L., Han, Y. and Hua, X. 2007. *Eperythrozoon* infection identified in an unknown aetiology anaemia patient. *Ann. Microbiol.* **57**: 467–469. [CrossRef]

DE GRUYTER
OPEN

Bull Vet Inst Pulawy 58, 375-378, 2014
DOI: 10.2478/bvip-2014-0058

Haemotropic mycoplasma infection revealed by real-time PCR in specific pathogen-free rats

Hinako Sashida, Ryô Harasawa, Toshihiro Ichijo, Hiroshi Satoh, Kazuhisa Furuhama

Cooperative Department of Veterinary Medicine, Iwate University, 3-18-8 Ueda, Morioka 020-8550, Japan
furuhama@iwate-u.ac.jp

Received: February 13, 2014 Accepted: August 06, 2014

Abstract

The presence of *Mycoplasma haemomuris* (haemoplasma) in blood samples collected from specific pathogen-free (SPF) laboratory rats bred in Japan was reported. Its presence was examined in Fischer 344, Sprague-Dawley (SD), and Wistar rat strains of both sexes by real-time PCR. All strains were positive for *M. haemomuris* infection. The 16S rRNA gene of *M. haemomuris* strain detected in the animals was amplified using end-point PCR. Only the entire nucleotide sequence of 16S rRNA gene of a mycoplasma strain detected in SD rats was determined and compared to those of other haemoplasmas. Our investigations suggest a wide *M. haemomuris* infection among the SPF rats purchased from commercial breeders in Japan.

Keywords: rat, specific pathogen free state, *Mycoplasma haemomuris*.

Introduction

It has long been recognised that most of the laboratory rats are carrying *Mycoplasma haemomuris* (formerly *Bartonella muris* or *Haemobartonella muris*). Latent infection of this haemotropic parasite (haemoplasma), an aetiological agent of infectious anaemia or splenomegaly in rodents, may undermine the validity of various animal experiments (2). Certain inbred rats, including Fischer 344 (F344), Sprague-Dawley (SD) and Wistar strains maintained in USA, Italy, and UK have been probably infected with *M. haemomuris* (3, 6, 8, 13). However, no examination has been documented in other countries up till now. Therefore, the presence of haemoplasma infection in specific pathogen-free (SPF) rats raised by commercial breeders in Japan was examined. Haemoplasma species have been identified solely on the basis of nucleotide sequences of the 16S rRNA or RNase P RNA genes, because of lack of appropriate means to cultivate them *in vitro* (7).

Material and Methods

Animals and specimens. Twenty-two anti-coagulated blood samples were collected under ethyl ether anaesthesia from SPF rats of F344 (n = 2), SD (n = 18), and Wistar (n = 2) strains of both sexes. All animals were purchased from a commercial breeder in Japan, and subjected to experiments immediately after receipt, without housing in our facility. The protocol used in the present study was approved by the Animal Care and Use Committee of Iwate University (Morioka, Japan), and all animal experiments were performed in accordance with the Guidelines for Care and Use of Laboratory Animals established by the Committee. Total DNA was extracted from 200 μL of blood samples using the QIAamp DNA Blood Mini Kit (Qiagen, Germany).

Analysis. To detect haemoplasmas, haemoplasma specific PCR primers for the 16S rRNA gene were used, as described elsewhere (9). Real-time PCR was performed using a SmartCycler (Cepheid, USA) with SYBR Premix Ex *Taq* (TaKaRa Bio., Japan).

The reaction mixture contained: 0.2 µL of each primer (50 pmol/µL); 12.5 µL of 2X SYBR Premix Ex *Taq*; and distilled water to a volume of 23 µL. Finally, 200 pg of a DNA sample was added to this mixture as a template. Amplification was achieved with 40 cycles of denaturation at 95°C for 5 s, annealing at 57°C for 20 s, and elongation at 72°C for 15 s, after the initial denaturation at 94°C for 30 s.

Afterwards end-point PCR was performed to determine the nucleotide sequence of the 16S rRNA gene. The end-point PCR was conducted with 50 µL of reaction mixtures each containing: 1 µL (100 pg) of DNA solution; 0.8 µL (one unit) of Tks Gflex DNA polymerase (TaKaRa Bio., Japan); 25 µL of 2X Gflex PCR buffer; 0.2 µL (50 pmol/µL) each of the forward primer (5'-AGAGTTTGATCCTGGCTCAG-3') and the reverse primer (5'-TACCTTGTTACGACTTA ACT-3'), and water to a final volume of 50 µL. After the initial denaturation at 94°C for 5 min, the reaction cycle was conducted 35 times with denaturation at 98°C for 10 s, annealing at 55°C for 60 s, extension at 68°C for 30 s, and final extension at 68°C for 5 min in a thermal cycler. The PCR product was fractionated on horizontal, submerged 1.0% agarose gels in TAE buffer (40 mM Tris, pH 8.0, 5 mM sodium acetate, 1 mM disodium ethylenediaminetetraacetate) at 100 volts for 30 min. After electrophoresis, the gels were stained in ethidium bromide solution (0.4 µg/mL) for 15 min and visualised under a UV transilluminator. DNA was extracted using a NucleoSpin Extract II kit (Macherey-Nagel, Germany) and was subjected to a direct sequencing in a 3500 Genetic Analyzer (Applied Biosystems, USA).

To identify the haemoplasma species, the 16S rRNA gene sequence of a haemoplasma strain detected in the SD rat was compared to other haemoplasma sequences from the DNA database using the Clustal W software (12). Phylogenetic tree generated using the neighbour-joining method (11) from a distance matrix was corrected for nucleotide substitutions using the Kimura two-parameter model (5).

Results

All the samples collected from the SPF rats were positive by the real-time PCR using haemoplasma-specific primers. Melting temperature of the PCR products was shown as a single peak at 85.92 ±0.16°C (Fig. 1). Using the end-point PCR, a band of approximately 1 kbp was produced from haemoplasmas detected in the SD rats by agarose gel electrophoresis (data not shown). The nucleotide sequences of the 16S rRNA gene from haemoplasma strains detected in SD rats of both sexes were successfully determined, though nucleotide sequencing of other strains was incomplete due to unknown reason. Both the nucleotide sequences from the two haemoplasma strains, SD001 detected in a male rat and SD002 in a female rat, were identical (100% similarity) in duplicate sequencings. No sex difference was noted.

The phylogenetic tree indicated that the haemoplasma strains detected in SD rats belonged to *M. haemomuris* (Fig. 2). The 16S rRNA gene nucleotide sequences of haemoplasma strains detected in the SD rat had 98.9% identity to that of *M. haemomuris* (10), which was supported by a high bootstrap value of 1000 in a phylogenetic tree. The SD002 sequence for the phylogenetic analysis was used because it is identical to SD001, and it identified them as *M. haemomuris*.

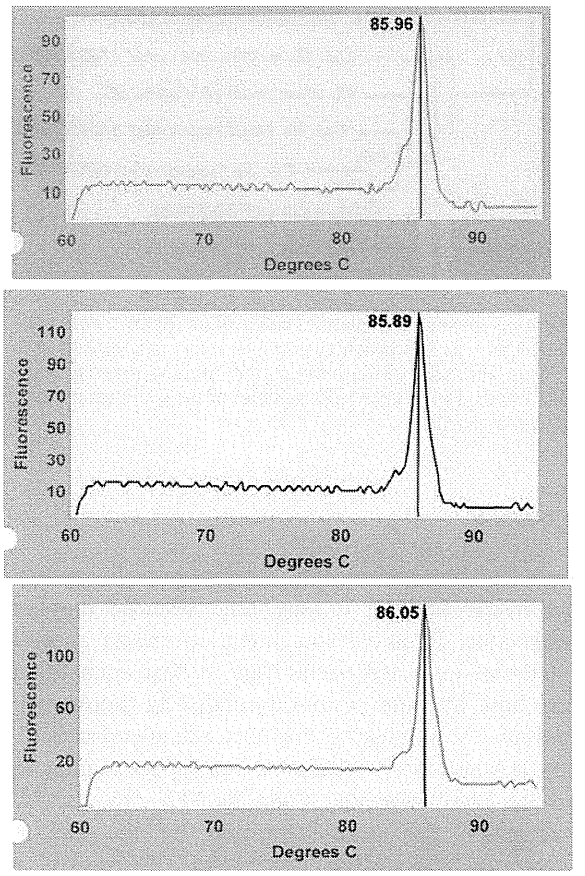

Fig. 1. Melting curve analyses for the real-time PCR products from the 16S rRNA gene of the haemoplasma strain detected in peripheral blood of SPF inbred rats. After real-time PCR, the melting experiment was performed from 60°C to 95°C at 0.2°C/s. Melting temperatures (*Tm*) of the PCR products of a haemoplasma strain detected in SD (top), F344 (middle), and Wistar (bottom) rats were depicted as a single peak at 85.96°C, 85.89°C, and 86.05°C respectively. Out of the 22 blood samples tested using real-time PCR, all were found to be positive for infection and their *Tm* values were 85.92 ± 0.16°C

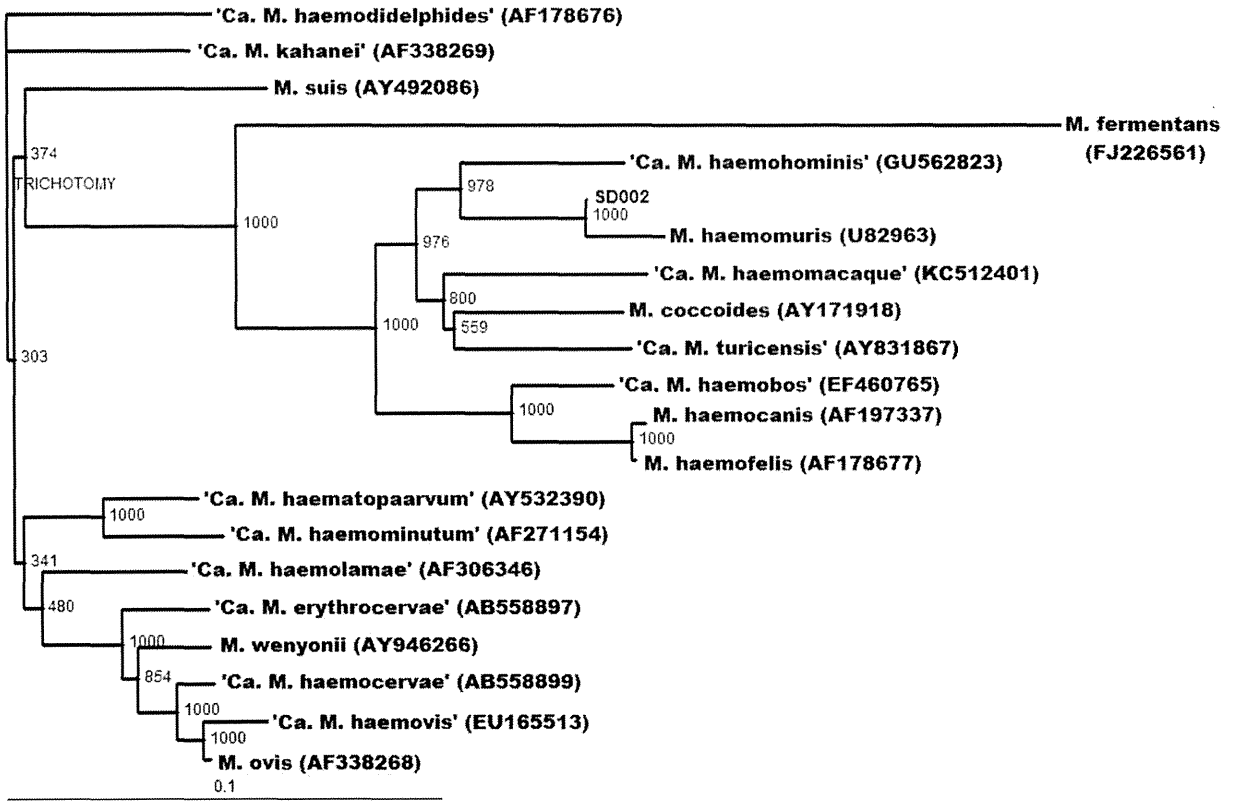

Fig. 2. Comprehensive neighbour-joining phylogenetic tree generated by the nucleotide sequences of 16S rRNA genes showing the evolutionary relationship among haemoplasmas and a strain (SD002) detected in a SD rat. The SD002 sequence was used because it is identical to that of SD001 in this tree. Accession numbers are shown in a parenthesis. *Mycoplasma fermentans* PG18, represented by FJ226561, was included as an out-group. The data was re-sampled 1000 times to generate bootstrap values indicated at the branch points. The tree is drawn to scale, with branch lengths in the same units as those of the evolutionary distances that were used to infer the phylogenetic tree (scale bar, 0.1 nucleotide substitutions per site)

Discussion

Haemoplasmas in SPF laboratory animals have been overlooked for a long time because they are uncultivable. Haemoplasma infection causes anaemia by immune-mediated haemolysis in host animals and alters host immune system by inducing autoimmune condition by mimicking the host cell membrane (3). Thus, it is necessary to examine haemoplasma infection prior to immunological study in SPF rats, but the investigation has been hampered by the lack of appropriate diagnostic procedures. Diagnosis of haemoplasma infection depended on cytological identification of the organisms on blood smears; however, this method has a low sensitivity and may misidentify the haemoplasmas as Howell-Jolly or Heinz bodies.

Although the infection route was unknown, blood-feeding arthropods, including a louse, have been considered to be the most probable source (4). However, the possibility of transplacental transmission remains as an open question because haemoplasma infections were reported in rat colonies free of ectoparasites (1, 3). In the current investigation, using haemoplasma-specific real-time PCR (9), SPF rats upon receipt from an accredited Japanese breeder facilitated with a strict barrier system, which can eliminate possible transmission by arthropod vectors, were examined.

To identify the haemoplasma species, the 16S rRNA gene sequence of a haemoplasma strain detected in the SD rat was compared to other haemoplasma sequences from the DNA database using Clustal W (12). A phylogenetic tree (Fig. 2) was generated using the neighbour-joining method (11) from a distance matrix corrected for nucleotide substitutions using the Kimura two-parameter model (5). The 16S rRNA gene nucleotide sequences of haemoplasma strains detected in the SD rat had 98.9% identity to that of *M. haemomuris* (10), which was supported by a high bootstrap value of 1000 in a phylogenetic tree. The SD002 in the tree was used, because SD001 and SD002 were considered to be the same strain derived from SPF inbred rats, which have been expected to be identical or no significantly different.

The real-time PCR to detect a haemoplasma infection in SPF rats bred in Japan, was applied. The phylogenetic analysis of the 16S rRNA gene demonstrated that a haemoplasma strain in SPF rats was identified as *M. haemomuris*. The nucleotide

sequence of the 16S rRNA gene of a haemoplasma strain detected in SD rats has been deposited to the DNA database under the accession number AB820289. Although, the determination of the nucleotide sequence of the 16S rRNA gene of a haemoplasma strain detected in the SD strain was only successful, F344 and Wistar strains may also be infected with the same strain due to almost the same *Tm* value obtained in the melting experiments.

In conclusion, haemotropic mycoplasma infections in SPF laboratory rats, which may influence the results of animal experiments, were confirmed. The haemoplasma examination by real-time PCR prior to animal experiments using SPF inbred rats, is recommended.

Acknowledgment: We thank Kazuya Nagai of the Cryobiofrontier Research Center, Iwate University, for his assistance in nucleotide sequencing.

References

1. Amici D., Murri O., Paparelli M, Tedeschi G.G.: Transmissione della *Haemobartonella muris* della madre al feto. Boll Soc Ital Biol Sper 1966, 42, 1501–1503.
2. Baker H.J., Cassell G.H., Lindsey J.R.: Research complications due to *Haemobartonella* and *Eperythrozoon* infections in experimental animals. Am J Pathol 1971, 64, 625–652.
3. Bartlett R., Pease P.: Latent *Haemobartonella muris* infection: its transmission and decline in an inbred, ectoparasite–free strain of Wistar rat. Parasitology 1975, 71, 35–40.
4. Crystal M.M.: The mechanism of transmission of *Haemobartonella muris* (Mayer) of rats by the spined rat louse, *Polyplax spinulosa* (Burmeister). J Parasitol 1958, 44, 603–606.
5. Kimura M.: A simple method for estimating evolutionary rates of base substitutions through comparative studies of nucleotide sequences. J Mol Evol 1980, 16, 111–120.
6. Kreier J.P., Hall L.: The relationship of parasitemia to the life span of erythrocytes of rats infected with *Haemobartonella muris*. J Infect Dis 1968, 118, 443–448.
7. Messick J.B.: Hemotrophic mycoplasmas (hemoplasmas): a review and new insights into pathogenic potential. Vet Clin Pathol 2004, 33, 2–13.
8. Moore D.H., Arison R.N., Tanaka H., Hall W.T., Chanowitz M.: Identity of the filterable hemolytic anemia agent of Sacks with *Haemobartonella muris*. J Bacteriol 1965, 90, 1669–1674.
9. Nishizawa I., Sato M., Fujihara M., Sato S., Harasawa R.: Differential detection of hemotropic *Mycoplasma* species in cattle by melting curve analysis of PCR products. J Vet Med Sci 2010, 72, 1704.
   Rikihisa Y., Kawahara M., Wen B., Kociba G., Fuerst P., Kawamori F., Suto C., Shibata S., Futohashi M.: Western immunoblot analysis of *Haemobartonella muris* and comparison of 16S rRNA gene sequences of *H. muris, H. felis,* and *Eperythrozoon suis*. J Clin Microbiol 1997, 35, 823–829.
10. Saitou N., Nei M.: The neighbor–joining method: a new method for reconstructing phylogenetic trees. Mol Biol Evol 1987, 4, 406–425.
11. Thompson J.D., Higgins D.G., Gibson T.J.: CLUSTAL W: improving the sensitivity of progressive multiple sequence alignment through sequence weighting, position–specific gap penalties and weight matrix choice. Nucleic Acids Res 1994, 22, 4673–4680.
12. Woods R., Parbhoo S.P.: Haemolytic anaemia in the Gunn rat following transplantation of isolated hepatocytes injected with *Haemobartonella muris*. Br J Exp Pathol 1981, 62, 8–12.

5. J. Widom, A. Klug, *Cell* **43**, 207–213 (1985).
6. J. P. Langmore, J. R. Paulson, *J. Cell Biol.* **96**, 1120–1131 (1983).
7. J. T. Finch, A. Klug, *Proc. Natl. Acad. Sci. U.S.A.* **73**, 1897–1901 (1976).
8. C. L. Woodcock, L. L. Frado, J. B. Rattner, *J. Cell Biol.* **99**, 42–52 (1984).
9. S. P. Williams *et al.*, *Biophys. J.* **49**, 233–248 (1986).
10. M. F. Smith, B. D. Athey, S. P. Williams, J. P. Langmore, *J. Cell Biol.* **110**, 245–254 (1990).
11. H. G. Davies, J. V. Small, *Nature* **217**, 1122–1125 (1968).
12. L. M. Carruthers, C. Tse, K. P. Walker 3rd, J. C. Hansen, *Methods Enzymol.* **304**, 19–35 (1999).
13. P. T. Lowary, J. Widom, *J. Mol. Biol.* **276**, 19–42 (1998).
14. P. J. Robinson, L. Fairall, V. A. Huynh, D. Rhodes, *Proc. Natl. Acad. Sci. U.S.A.* **103**, 6506–6511 (2006).
15. B. Dorigo *et al.*, *Science* **306**, 1571–1573 (2004).
16. T. Schalch, S. Duda, D. F. Sargent, T. J. Richmond, *Nature* **436**, 138–141 (2005).
17. F. Thoma, T. Koller, A. Klug, *J. Cell Biol.* **83**, 403–427 (1979).
18. J. O. Thomas, *Curr. Opin. Cell Biol.* **11**, 312–317 (1999).
19. D. L. Bates, J. O. Thomas, *Nucleic Acids Res.* **9**, 5883–5894 (1981).
20. J. Allan, P. G. Hartman, C. Crane-Robinson, F. X. Aviles, *Nature* **288**, 675–679 (1980).
21. D. Z. Staynov, *Bioessays* **30**, 1003–1009 (2008).
22. T. D. Frouws, H. G. Patterton, B. T. Sewell, *Biophys. J.* **96**, 3363–3371 (2009).
23. K. Luger, A. W. Mäder, R. K. Richmond, D. F. Sargent, T. J. Richmond, *Nature* **389**, 251–260 (1997).
24. S. H. Syed *et al.*, *Proc. Natl. Acad. Sci. U.S.A.* **107**, 9620–9625 (2010).
25. D. Z. Staynov, C. Crane-Robinson, *EMBO J.* **7**, 3685–3691 (1988).
26. B. R. Zhou *et al.*, *Proc. Natl. Acad. Sci. U.S.A.* **110**, 19390–19395 (2013).
27. G. J. Carter, K. van Holde, *Biochemistry* **37**, 12477–12488 (1998).
28. L. Fan, V. A. Roberts, *Proc. Natl. Acad. Sci. U.S.A.* **103**, 8384–8389 (2006).
29. S. H. Leuba, C. Bustamante, K. van Holde, J. Zlatanova, *Biophys. J.* **74**, 2830–2839 (1998).
30. J. Bednar *et al.*, *Proc. Natl. Acad. Sci. U.S.A.* **95**, 14173–14178 (1998).
31. A. Routh, S. Sandin, D. Rhodes, *Proc. Natl. Acad. Sci. U.S.A.* **105**, 8872–8877 (2008).

Acknowledgments: This work was supported by grants from the National Basic Research Program of China (2010CB912400 to P.Z., 2011CB966300 to G.L., and 2009CB825500 to R.M.X. and P.Z.); the National Natural Science Foundation of China (91219202 to G.L., 31230018 to P.Z., 91019007 to G.L., 21261130090 to P.Z., and 31000566 to P.C.); Strategic Priority Research Program (XDA01010304 to G.L. and XDB08010100 to P.Z. and R.M.X.) and Key Research Program (KJZD-EW-L05 to P.Z., G.L., and R.M.X.) from the Chinese Academy of Sciences; and the Scientific Research Foundation for the Returned Overseas Chinese Scholars, State Education Ministry, to P.C. All EM data were collected and processed at the Center for Bio-imaging, Institute of Biophysics, Chinese Academy of Sciences. We thank G. Ji and X. Huang for their technical help and support with electron microscopy and L. Ling for technical help and support with the data processing in the High Performance Computing Service Station. We are also indebted to the colleagues whose work could not be cited because of the limitation of space. The cryo-EM maps for the 12 × 177 bp, 12 × 187 bp and 24 × 177 bp chromatin fibers were deposited into the Electron Microscopy Data Bank with the accession codes EMD-2600, EMD-2601 and EMD-2602, respectively. The authors declare no conflicts of interest.

Supplementary Materials

www.sciencemag.org/content/344/6182/376/suppl/DC1
Materials and Methods
Figs. S1 to S8
References (*32–41*)
Movies S1 to S3

28 January 2014; accepted 18 March 2014
10.1126/science.1251413

Genome Sequence of the Tsetse Fly (*Glossina morsitans*): Vector of African Trypanosomiasis

International *Glossina* Genome Initiative*†

Tsetse flies are the sole vectors of human African trypanosomiasis throughout sub-Saharan Africa. Both sexes of adult tsetse feed exclusively on blood and contribute to disease transmission. Notable differences between tsetse and other disease vectors include obligate microbial symbioses, viviparous reproduction, and lactation. Here, we describe the sequence and annotation of the 366-megabase *Glossina morsitans morsitans* genome. Analysis of the genome and the 12,308 predicted protein–encoding genes led to multiple discoveries, including chromosomal integrations of bacterial (*Wolbachia*) genome sequences, a family of lactation-specific proteins, reduced complement of host pathogen recognition proteins, and reduced olfaction/chemosensory associated genes. These genome data provide a foundation for research into trypanosomiasis prevention and yield important insights with broad implications for multiple aspects of tsetse biology.

African trypanosomiasis is transmitted by the tsetse fly to humans (sleeping sickness) and livestock (nagana) throughout sub-Saharan Africa, with an estimated 70 million people at risk of infection. Rearing livestock in endemic areas is difficult to impossible and results in an economic loss in agricultural output of several billion U.S. dollars per year. Human infections are fatal if untreated, but tools for disease control are limited because it has not been possible to develop vaccines and current trypanocidal drug treatments result in undesirable side effects with growing reports of drug resistance. The reduction or elimination of tsetse populations is an effective method for disease control that could be improved with greater knowledge of their biology and genetics (*1*).

Tsetse flies are key representatives of the dipteran clade Calyptratae, which represents 12% of the known diversity within the dipteran order. Many of the calyptrate species are blood feeders of biomedical importance (*2*). In addition, members of the calyptrate family of Glossinidae and superfamily Hippoboscoidea, to which tsetse belong (fig. S1) (*3*), are defined by the ability to nourish intrauterine offspring from glandular secretions and give birth to fully developed larvae (obligate adenotrophic viviparity). Tsetse flies live considerably longer than other vector insects, which somewhat compensates for their slow rate of reproduction. Trypanosome infections in tsetse are acquired by blood feeding from an infected vertebrate host, and trypanosomes have to overcome multiple immune barriers to establish an infection within the fly. As a result, trypanosome infection prevalence is low in field populations and in experimentally infected tsetse (*4*). Tsetse have symbionts that compensate for their nutritionally restricted diet by the production of specific metabolites and influence multiple other aspects of the fly's immune and reproductive physiology (*5*).

In 2004, the International *Glossina* Genome Initiative (IGGI) was formed (*6*) to expand research capacity for *Glossina*, particularly in sub-Saharan Africa, through the generation and distribution of molecular resources, including bioinformatics training. An outcome of the effort undertaken by IGGI is the annotated *Glossina morsitans* genome presented here and further developed in satellite papers on genomic and functional biology findings that reflect the unique physiology of this disease vector (*7–14*).

Characteristics of the *Glossina* Genome

A combination of sequencing methods were used to obtain the *Glossina morsitans morsitans* (*Gmm*) genome, including Sanger sequencing of bacterial artificial chromosomes (BACs), small-insert plasmid and large-insert fosmid libraries, and 454 and Illumina sequencing (tables S1 and S2). The sequences were assembled into 13,807 scaffolds of up to 25.4 Mb, with a mean size of 27 kb and half the genome present in scaffolds of at least 120 kb. The 366-Mb genome is more than twice the size of the *Drosophila melanogaster* genome (fig. S2A and table S3). Clear conservation of synteny was detected between *Glossina* and *Drosophila*, but with the blocks of synteny tending to be twice as large in *Glossina* due to larger introns and an increase in the size of intergenic sequences, possibly as a result of transposon activity and/or repetitive sequence expansions. Sequences from most of the major groups of retrotransposons and DNA transposons are found in the *Glossina* genome (table S4). These sequences comprise ~14% of the assembled genome, in contrast to 3.8% of the *Drosophila*

*Members of the International *Glossina* Genome Initiative, affiliations, and individual contributions appear at the end of this paper.
†Corresponding author. E-mail: serap.aksoy@yale.edu (Serap Aksoy); geoffrey.attardo@yale.edu (G.M.A.); mb4@sanger.ac.uk (M.B.)